Nature of Bonding in the Thermal Cyclization of (Z)-1,2,4,6-Heptatetraene and Its Heterosubstituted Analogues

Eduardo E. Chamorro*

Departamento de Ciencias Químicas, Facultad de Ecología y Recursos Naturales, Universidad Andrés Bello, Avenida República 275, Santiago, Chile

Rafael Notario

Instituto de Química Física "Rocasolano", Consejo Superior de Investigaciones Científicas (C.S.I.C), Serrano 119, 28006 Madrid, España

Received: January 12, 2004; In Final Form: February 25, 2004

The topological analysis of the electron localization function (ELF), a measure of local Pauli repulsion and an orbital-independent technique for bonding analysis, has been applied to explore further the intriguing nature of bonding at the transition states (TSs) of the thermal electrocyclization of (*Z*)-1,2,4,6-heptatetraene and its heterosubstituted analogues, (2*Z*)-2,4,5-hexatrienal and (2*Z*)-2,4,5-hexatrien-1-imine. In the context of the relevant controversy concerning the pericyclic or pseudopericyclic intimate nature of bonding at these TSs (De Lera, A. R.; Alvarez, R.; Lecea, B.; Torrado, A.; Cossío, F. P. *Angew. Chem., Int. Ed*. **2001**, 40, 557; Rodríguez-Otero, J.; Cabaleiro-Lago, E. M. *Angew. Chem., Int. Ed*. **2002**, 41, 1147; De Lera, A. R.; Cossío, F. P. *Angew. Chem., Int. Ed*. **2002**, 41, 1150; Rodriguez-Otero, J.; Cabaleiro-Lago, E. M. *Chem.—Eur. J*. **2003**, 9, 1837), we show for the first time that the analysis based on ELF provides further evidence in support of a single disrotatory pericyclic bond interaction in the three cases. This conclusion arises from an examination of the fluctuation of electron density at the cyclic reaction center.

Introduction

A very interesting controversy concerning the intimate nature of bonding at the transition states for the thermal cyclization of (*Z*)-1,2,4,6-heptatetraene (**C**) and its heterosubstituted analogues, (2*Z*)-2,4,5-hexatrienal (**B**) and (2*Z*)-2,4,5-hexatrien-1-imine (**A**), has been raised recently.[1,2] Two possible routes, as it is represented in Scheme 1, have been postulated: a pericyclic disrotatory electrocyclization via transition state TS1 and a pseudopericyclic nucleophilic addition of the heteroatom lone pair via transition state TS2. The distinction among these orbital topologies becomes relevant because in pseudopericyclic reactions the orbital overlap around the ring of breaking and forming bonds is absent, allowing planar TS geometries with very low activation barriers along the complete reaction paths, an aspect of importance in the design of new synthetic routes.[3]

De Lera et al.[1] carried out the first theoretical examination of the mechanism of reactions for **A**, **B**, and **C** systems, selected as model reactions of the thermal cyclizations of (2*Z*)-2,4,5-hexatrienals and their Schiff bases. In work carried out on the basis of the examination of nuclear motion along the imaginary frequency at the TS and also from computed nucleus-independent chemical shifts (NICS) associated with the aromatic character of structures,[4] they conclude that there are fundamental differences among the processes studied: the thermal cyclization of **C** occurs via a disrotatory electrocyclization with a pericyclic and aromatic TS1, and the cyclizations of heterosubstituted analogues **A** and **B** involve a nucleophilic addition of the heteroatom lone pair to the sp-hybridized carbon atoms through a pseudopericyclic and not an aromatic TS2.

SCHEME 1: Suggested Reaction Mechanisms for the Thermal Cyclization of (Z)-1,2,4,6-Heptatetraene and Its Heterosubstituted Analogues via a Pericyclic Disrotatory Pathway (TS1) or through Pseudopericyclic Nucleophilic Addition (TS2)

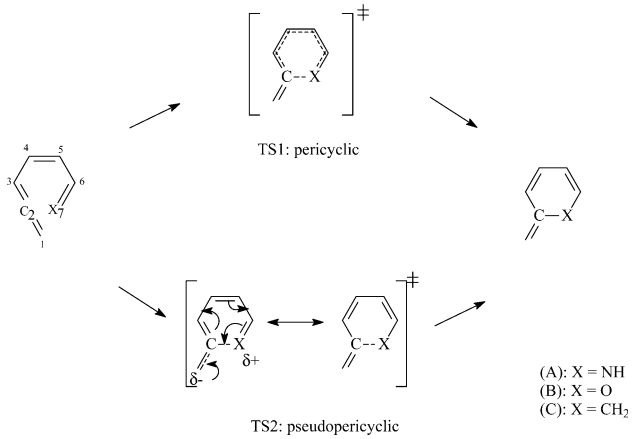

Rodriguez-Otero and Cabaleiro-Lago[2a] have questioned the results of De Lera et al.[1] concerning the pseudopericyclic nature of the cyclization of (2*Z*)-2,4,5-hexatrien-1-imine (**A**) and (2*Z*)-2,4,5-hexatrienal (**B**). Their analysis yields the conclusion that the three processes studied are essentially disrotatory pericyclic electrocyclizations even though they are assisted by the electron lone pair on the heteroatom. De Lera and Cossío[2b] have replied that these findings are based on a critical reexamination of the movement along the imaginary frequency, the charge accumulation at the C1 center, and considerations of the aromaticity of TS structures based on NICS values. However, very recently,

* Corresponding author. E-mail: echamorro@unab.cl. Tel: 56-2-6618229. Fax: 56-2-6618269.

10.1021/jp049847y CCC: $27.50
Published on Web 04/14/2004

Rodriguez-Otero and Cabaleiro-Lago have reported[5] new studies centered around the determination of magnetic properties as the basis to estimate the aromatic character of TSs. NBO data analysis throughout the reaction path of the three reactions has also been reported to confirm the existence of some charge accumulation at the C7 center. Comparisons with the cyclization of 5-oxo-2,4-pentadienal, certainly a pseudopericyclic process,[6] suggested that although the lone electron pair on the heteroatom in **A** and **B** seemingly plays a crucial role in the reaction mechanism the pathway must be understood in terms of a pericyclic disrotatory electrocyclization.

It is clear, from the above-reported evidence, that the intimate nature of bonding at these TSs and related thermal processes remains open to further studies. With the aim of searching for more insight concerning the nature of the electronic rearrangement in these systems, we have exploited the usefulness of the topological analysis of the electron localization function (ELF), a robust technique of bonding analysis. The ELF constitutes a measure of the local (i.e., position-dependent) Pauli repulsion.[7,8] It is known that on the basis of primary and/or secondary interactions between orbitals the fundamental difference among pericyclic and pseudopericyclic topologies is the conservation or nonconservation, respectively, of a cyclic overlap between the array of orbitals that are involved in bonding changes at the transition state.[3] The topological analysis of the ELF could provide further insights into these differences. In this context, we have recently presented[9] results from an ongoing systematic study concerning the characterization of bonding at pericyclic and pseudopericyclic transition states of chelotropic decarbonylations using the ELF analysis. This tool has been shown to be a simple descriptor of the electronic rearrangement for these fundamental types of chemical reactions. It has been shown that the lack of cyclic "orbital" overlap in pseudopericyclic reactions can be related to the specific pattern of fluctuation in electron populations among the ELF basins. It should be noted that this type of analysis yields a picture of bonding for pericyclic and/or pseudopericyclic reactions that is not based on orbital concepts of bonding. However, it was already known that there is a clear relation between the ELF and the nodal orbital structure of molecules and solids.[10] Furthermore, the topological analysis of the ELF constitutes a robust technique of bonding characterization almost independent of the method of calculation,[8c] which provides a suitable wave function. Earlier studies on the benchmark pericyclic reactions corresponding to the [1_s,3_a]-hydrogen, [1_a,3_s]-methyl, and [1_a,3_s]-fluorine sigmatropic shifts in the allyl system have also emphasized the usefulness of the analysis of properties of the electron density integrated over the ELF basins.[11] A consistent picture of bonding, which seems to be of complementary value to the traditionally used Woodward−Hoffmann analysis, will be expected from this scheme of analysis.

Results and Discussion

Following refs 1 and 2 for comparison purposes, transition states for the electrocyclizations of **A**, **B**, and **C** have been optimized at the B3LYP/6-31+G(d) level of theory. This level is suitable enough to provide a good wave function for our problem at hand. Geometry optimization calculations were made using the Gaussian 98 package of programs.[12] The topological analysis of the ELF has been done using the TopMod programs[13,14] and the Vis5d[15] visualization tools.

Below, we first review shortly some general aspects of the ELF analysis that are of particular interest in the present work. In the spirit of more detailed discussions, the reader is referred to widely available reviews on this powerful technique of bonding analysis.[7,8]

Topological Analysis of the Electron Localization Function. The topological analysis of the electron localization function (ELF), $\eta(\mathbf{r})$,[7] first introduced by Savin and Silvi,[8] provides us with a useful and convenient partitioning of the molecular space into regions that are associated with chemically meaningful concepts such a atomic cores, bonds, and lone pairs. Each such region or basin is related to a local maximum (i.e., an attractor) of the ELF function. The scaled (within the [0, 1] interval) local-function ELF was defined by Becke and Edgecombe[7] in the framework of the Taylor expansion characterization of the pair density function $P(\mathbf{r}, s) = {}^1/_2 s^2 T(\mathbf{r}) + ...$ Henceforth, the function $\eta(\mathbf{r})$ can be written and interpreted in terms of the excess local kinetic energy density due to Pauli repulsion, $T(\mathbf{r})$, and the Thomas−Fermi kinetic energy density, $T_h(\mathbf{r})$:[8]

$$\eta(\mathbf{r}) = \left[1 + \left[\frac{T(\mathbf{r})}{T_h(\mathbf{r})}\right]^2\right]^{-1} \tag{1}$$

In this way, ELF basins can be consistently associated with bonding entities in the framework of a fundamental and unified description of chemical bonding because the $\eta(\mathbf{r})$ local function is directly related to the pairing of electrons through the Pauli exclusion principle.[8] Given the definition in eq 1, the ELF will acquires values close to 1 where parallel spins are highly avoided (i.e., in lone pairs or bond regions), whereas it will be close to zero near the boundaries between two such pair regions. The homogeneous electron gas is taken only as a reference for normalization in eq 1. Consistent with the Lewis theory, we can identify the basins from the topological analysis of the ELF with core (i.e., atomic) and valence (i.e., bonds or lone pair regions) regions labeled $C(X_1)$ and $V(X_1, X_2,...)$, respectively, where X_1 and X_2 stand for the atomic centers. Also, consistent nomenclature can be used to describe multicenter bonds and their interactions: the number of core basins sharing a common boundary defines the synaptic order of each valence basin, allowing us to describe lone pairs as monosynaptic, two-center bonds as disynaptic, three-center bonds as trisynaptic, and so on.

For a single-determinant wave function, eq 1 can be straightforwardly evaluated in terms of electron density $\rho(\mathbf{r})$:

$$T(\mathbf{r}) = \frac{1}{2}\sum_i |\nabla\varphi_i(\mathbf{r})|^2 - \frac{1}{8}\frac{|\nabla\rho(\mathbf{r})|^2}{\rho(\mathbf{r})}$$

$$T_h(\mathbf{r}) = 2.871\rho(\mathbf{r})^{5/3}$$

and

$$\rho(\mathbf{r}) = \sum_i |\varphi_i(\mathbf{r})|^2 \tag{2}$$

where atomic units are implicit in this formulation, and $\varphi_i(\mathbf{r})$ are the Hartree−Fock (HF) or Kohn−Sham (KS) orbitals. Henceforth, the basins of attractors, derived from the gradient field of the ELF function given in eq 1, and their properties are correlated with pair-region characteristics in the molecular system. In this context, these properties are interpreted on the basis of intuitive ideas and concepts of the localization and delocalization of electron density.[16] Quantitative analysis is performed through a standard topological population technique arising from the integration of density $\rho(\mathbf{r})$ and second-order

TABLE 1: Basin Populations, $\tilde{N}_i$, Standard Deviations, $\sigma^2(\tilde{N}_i)$, Relative Fluctuations, $\lambda(\tilde{N}_i)$, and Main Contributions of Other Basins, i(%), to $\sigma^2(\tilde{N}_i)$ for Transition State A from the Density Obtained at the B3LYP/6-31+G(d) Level of Theory

	basin	$\tilde{N}_i$	$\sigma^2(\tilde{N}_i)$	$\lambda(\tilde{N}_i)$	contribution analysis (%)
1	V(H1, C1)	2.08	0.67	0.32	**2** (27.4), **3** (23.6), **4** (26.2), **5** (4.9)
2	V(H2, C1)	2.04	0.67	0.33	**1** (27.3), **3** (23.8), **4** (26.1), **5** (5.2)
3	V(C1, C2)	1.88	1.05	0.56	**1** (15.0), **2** (15.2), **4** (27.0), **5** (18.9), **14** (6.3)
4	V(C1, C2)	1.93	1.05	0.54	**1** (16.7), **2** (16.7), **3** (27.1), **5** (20.2)
5	V(C2, C3)	3.43	1.50	0.44	**3** (13.2), **4** (14.0), **6** (18.6), **7** (20.0), **14** (6.0)
6	V(H3, C3)	2.08	0.68	0.33	**4** (3.5), **5** (41.1), **7** (28.3), **8** (3.8), **9** (3.2)
7	V(C3, C4)	2.47	1.21	0.49	**5** (25.0), **6** (16.0), **8** (15.7), **9** (20.9)
8	V(H4, C4)	2.12	0.65	0.31	**5** (3.9), **6** (3.9), **7** (29.1), **9** (38.7), **10** (4.5), **11** (3.3)
9	V(C4, C5)	3.19	1.45	0.45	**5** (3.1), **7** (17.4), **8** (17.4), **10** (19.1), **11** (19.9)
10	V(H5, C5)	2.13	0.67	0.31	**8** (4.4), **9** (41.5), **11** (27.6), **12** (3.4)
11	V(C5, C6)	2.44	1.17	0.48	**9** (24.6), **10** (15.7), **12** (16.0), **13** (17.2), **14** (4.8)
12	V(H6, C6)	2.16	0.65	0.30	**9** (4.3), **10** (3.5), **11** (28.7), **13** (32.1), **14** (9.0), **15** (5.0)
13	V(C6, N)	2.71	1.35	0.50	**11** (15.0), **12** (15.6), **14** (32.1), **15** (17.8)
14	V(N)	2.75	1.29	0.47	**3** (5.1), **5** (7.0), **11** (4.4), **12** (4.6), **13** (33.6), **15** (25.9)
15	V(H8, N)	1.99	0.76	0.38	**12** (4.3), **13** (31.8), **14** (44.1)

density matrices $\pi(\mathbf{r}_1, \mathbf{r}_2)$ in the volume of the ELF basins, Ω. The average population of a basin, $\tilde{N}_i$, is obtained from

$$\tilde{N}_i = \int_{\Omega_i} \rho(\mathbf{r})\, d\mathbf{r} \tag{3}$$

and their population variance, $\sigma^2(\tilde{N}_i)$ (i.e., the quantum uncertainty of the basin population) can be calculated as

$$\sigma^2(\tilde{N}_i) = \int_{\Omega_i} d\mathbf{r}_1 \int_{\Omega_i} d\mathbf{r}_2\, \pi(\mathbf{r}_1, \mathbf{r}_2) + \tilde{N}_i - [\tilde{N}_i]^2 = \sum_{i \neq j} B_{ij} = \sum_{i \neq j} - \int_{\Omega_i} d\mathbf{r}_1 \int_{\Omega_j} d\mathbf{r}_2\, \rho(\mathbf{r}_1)\, \rho(\mathbf{r}_2)\, h(\mathbf{r}_1, \mathbf{r}_2)\, d\mathbf{r}_2 \tag{4}$$

where $h(\mathbf{r}_1, \mathbf{r}_2)$ stands for the exchange-correlation hole.[8] Therefore, the $\sigma^2(\tilde{N}_i)$ describes the excess of the number of pairs resulting from the interaction of Ω_i with other basins. It becomes clear that the covariance analysis (i.e., fluctuation of electron populations) based on eq 6 represents a useful tool for the examination of the electronic delocalization pattern involving pairs of basins.[9,11] This is the main hypothesis in the present work. With the aim of dealing with delocalization (i.e., fluctuation), the B_{ij} term values have been divided by $\sigma^2(i, j)$ to obtain these contributions in percentages. Similarly, Bader's relative fluctuation $\lambda(\tilde{N}_i)$ index, an efficient tool for the study of delocalization,[16] is defined in terms of the above quantities,

$$\lambda(\tilde{N}_i) = \frac{\sigma^2(\tilde{N}_i)}{\tilde{N}_i} \tag{5}$$

Certainly, we must finally comment that several useful applications of these tools for the treatment of chemical bonds have been reported recently in many different fields of chemistry.[17] It is therefore generally accepted that topological-based analysis, particularly that pertaining to the covariance data, provides relevant physical and chemical insights concerning the general nature of bonding and electron delocalization in molecular systems.[18]

TABLE 2: Basin Populations, $\tilde{N}_i$, Standard Deviations, $\sigma^2(\tilde{N}_i)$, Relative Fluctuations, $\lambda(\tilde{N}_i)$, and Main Contributions of Other Basins, i(%), to $\sigma^2(\tilde{N}_i)$ for Transition State B from the Density Obtained at the B3LYP/6-31+G(d) Level of Theory

	basin	$\tilde{N}_i$	$\sigma^2(\tilde{N}_i)$	$\lambda(\tilde{N}_i)$	contribution analysis (%)
1	V(H1, C1)	2.08	0.67	0.32	**2** (27.6), **3** (23.8), **4** (25.5), **5** (4.5)
2	V(H2, C1)	2.05	0.67	0.33	**1** (27.6), **3** (24.3), **4** (25.7), **5** (4.5)
3	V(C1, C2)	1.92	1.05	0.55	**1** (15.2), **2** (15.5), **4** (27.3), **5** (17.5), **14** (5.3)
4	V(C1, C2)	1.93	1.04	0.54	**1** (16.5), **2** (16.6), **3** (27.5), **5** (19.1)
5	V(C2, C3)	3.19	1.45	0.46	**3** (12.7), **4** (13.7), **6** (17.8), **7** (22.3), **14** (4.8)
6	V(H3, C3)	2.09	0.68	0.32	**4** (3.4), **5** (38.1), **7** (31.7), **8** (3.7)
7	V(C3, C4)	2.66	1.29	0.48	**5** (25.1), **6** (16.7), **8** (15.7), **9** (18.6)
8	V(H4, C4)	2.12	0.65	0.31	**5** (4.1), **6** (3.9), **7** (31.3), **9** (34.8), **10** (4.1), **11** (4.6)
9	V(C4, C5)	2.86	1.34	0.47	**7** (17.9), **8** (16.8), **10** (17.3), **11** (23.9)
10	V(H5, C5)	2.13	0.67	0.31	**8** (4.0), **9** (34.8), **11** (35.0), **12** (3.8)
11	V(C5, C6)	2.78	1.32	0.47	**9** (24.4), **10** (17.8), **12** (15.8), **13** (12.0), **14** (4.1), **15** (4.2)
12	V(H6, C6)	2.19	0.65	0.30	**9** (4.4), **10** (3.9), **11** (32.0), **13** (22.4), **14** (6.3), **15** (11.9)
13	V(C6, O)	2.07	1.19	0.58	**11** (13.2), **12** (12.2), **14** (26.2), **15** (32.1)
14	V(O)	2.30	1.21	0.52	**3** (4.6), **5** (5.7), **11** (4.4), **12** (3.4), **13** (25.8), **15** (39.2)
15	V(O)	3.03	1.28	0.42	**11** (4.3), **12** (6.0), **13** (29.8), **14** (36.9)

TABLE 3: Basin Populations, $\tilde{N}_i$, Standard Deviations, $\sigma^2(\tilde{N}_i)$, Relative Fluctuations, $\lambda(\tilde{N}_i)$, and Main Contributions of Other Basins, i(%), to $\sigma^2(\tilde{N}_i)$ for Transition State C from the Density Obtained at the B3LYP/6-31+G(d) Level of Theory

	basin	$\tilde{N}_i$	$\sigma^2(\tilde{N}_i)$	$\lambda(\tilde{N}_i)$	contribution analysis (%)
1	V(H1, C1)	2.09	0.66	0.32	**2** (28.1), **3** (21.4), **4** (25.3), **5** (6.2)
2	V(H2, C1)	2.06	0.66	0.32	**1** (28.1), **3** (21.8), **4** (25.3), **5** (6.2)
3	V(C1, C2)	1.71	0.99	0.58	**1** (14.3), **2** (14.5), **4** (26.5), **5** (21.9), **14** (3.3)
4	V(C1, C2)	1.89	1.03	0.54	**1** (16.2), **2** (16.3), **3** (25.5), **5** (22.3)
5	V(C2, C3)	3.64	1.60	0.44	**3** (13.6), **4** (14.4), **6** (17.1), **7** (18.5), **13** (5.4)
6	V(H3, C3)	2.08	0.68	0.32	**4** (3.2), **5** (40.4), **7** (29.0), **8** (3.9), **9** (3.5)
7	V(C3, C4)	2.52	1.22	0.49	**5** (24.2), **6** (16.0), **8** (15.8), **9** (21.7)
8	V(H4, C4)	2.14	0.66	0.31	**5** (3.6), **6** (4.0), **7** (29.1), **9** (38.5), **10** (4.5)
9	V(C4, C5)	3.09	1.43	0.46	**5** (3.3), **7** (18.6), **8** (17.9), **10** (18.0), **11** (19.0)
10	V(H5, C5)	2.13	0.66	0.31	**8** (4.5), **9** (38.7), **11** (29.3), **12** (3.4), **13** (3.4)
11	V(C5, C6)	2.52	1.21	0.48	**9** (22.4), **10** (16.0), **12** (16.2), **13** (21.8)
12	V(H6, C6)	2.12	0.66	0.31	**9** (4.0), **10** (3.5), **11** (29.9), **13** (38.0), **14** (3.4), **15** (4.1)
13	V(C6, C7)	3.14	1.46	0.47	**5** (5.9), **11** (18.1), **12** (17.1), **14** (17.6), **15** (17.8)
14	V(H7, C7)	2.12	0.71	0.33	**3** (4.7), **5** (6.3), **11** (3.4), **12** (3.1), **13** (36.3), **15** (27.3)
15	V(H8, C7)	2.12	0.66	0.31	**5** (4.2), **11** (3.2), **12** (4.1), **13** (39.7), **14** (29.4)

Thermal Electrocyclization of (*Z*)-1,2,4,6-Heptatetraene and Its Heterosubstituted Analogues. The basin- and variance-related properties obtained from the ELF topological population analysis, including the basin populations, $\tilde{N}_i$, their associated variances, $\sigma^2(\tilde{N}_i)$, the relative fluctuation, $\lambda(\tilde{N}_i)$, and main contributions (in percent) from other basins, i(%), to $\sigma^2(\tilde{N}_i)$ for TS **A**, TS **B**, and TS **C**, have been reported in Tables 1−3, respectively. Because core basin populations and related properties do not play a relevant role in the description of the reactivity observed, only valence basin results have been included in the present analysis.

The examination of the gradient field of the ELF at the present level of theory reveals that there are not disynaptic basins associated directly with the C2 and X7 centers at TS **A**, TS **B**, and TS **C**. Consistent with such a type of reaction and reported

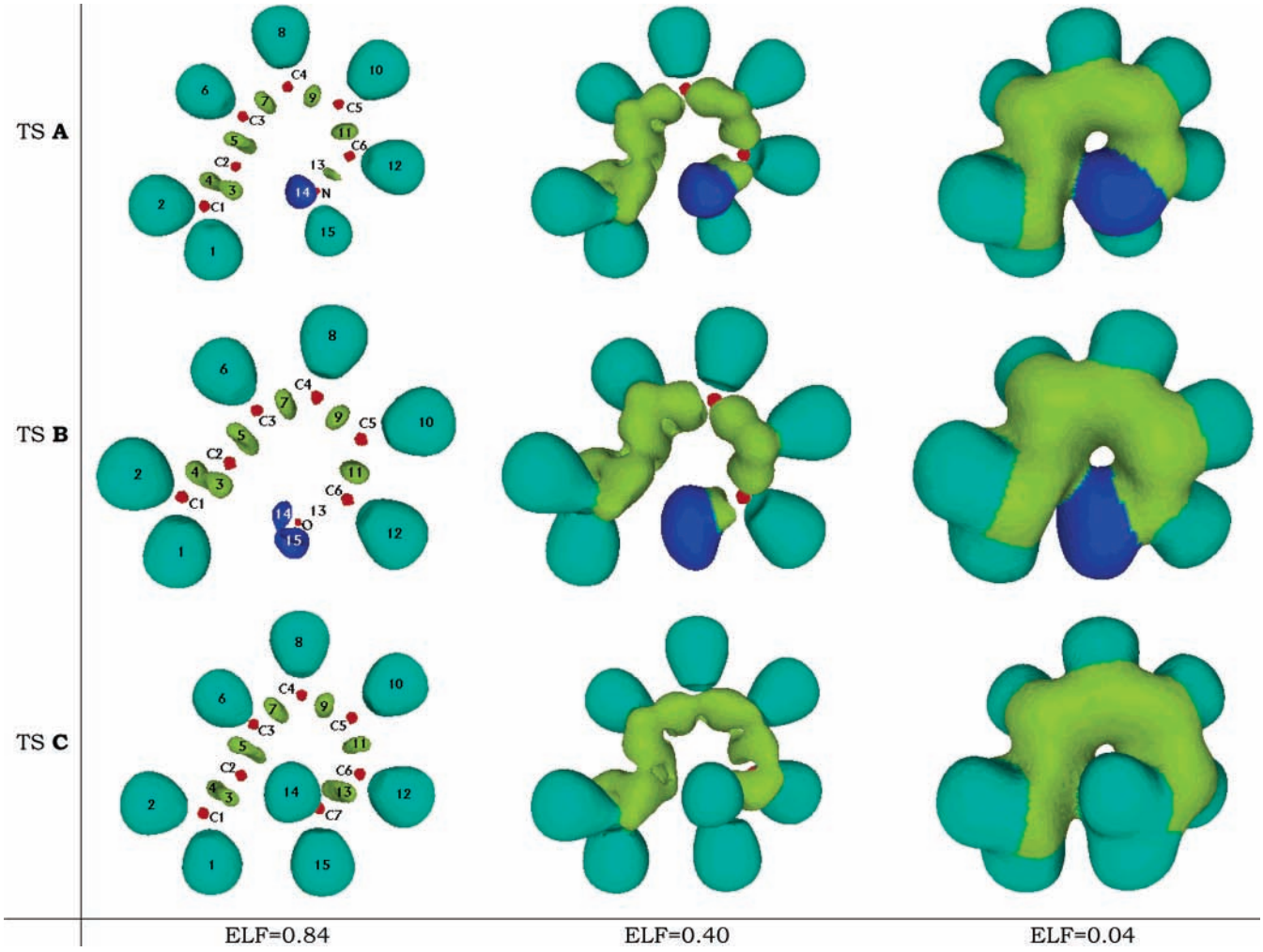

Figure 1. Localization domains of the electron localization function (ELF) at TS **A**, TS **B**, and TS **C** transition states (as calculated at ELF = 0.84, 0.40, and 0.04 isosurfaces) from the optimized wave functions at the B3LYP/6-31+G(d) level of theory. Core basins (C) are represented in red, valence protonated disynaptic basins V(C, H) are in green, valence disynaptic V(C, C) or V(C, X7) basins are in yellow-green, and valence monosynaptics associated with lone pair regions at N and O are in blue.

activation energies,[1] the electronic rearrangement along the reaction coordinate becomes "early" at the transition-state position. However, as will be discussed below, the pattern of fluctuation reveals explicitly that there exists a cyclic interaction involving the lone pair domains of localization at N and O in the TS **A** and TS **B** domains or the valence V(C6, C7) domain at TS **C** with the V(C2, C3) and V(C1, C2) valence domains.

The ELF results suggest that at the three TSs the bonding resembles classical, although highly asymmetric, pericyclic processes. Note from the fluctuation population reported in Tables 1−3 that the lone pair basin region on the N center at TS **A**, localizing 2.75e, contributes 6.0% to the V(C2, C3) valence basin population; the lone pair monosynaptic basin regions on the O center at TS **B**, localizing 2.30e and 3.03e each, do it in 4.8%. Lone pair populations in these two cases seem to play, as suggested by Rodriguez-Otero and Cabaleiro-Lago,[2a,5] only a stabilizing role in the global electrocyclization process. Similarly, the V(C6, C7) disynaptic basin population in the TS **C**, which localizes 3.14e, mainly contributes to the C2−C3 valence population in 5.4%. Note also that a direct fluctuation between the V(C6, N) and the V(C6, O) domains with the V(C2, C3) region is very low (<1.5%). These lone pair populations are also delocalized over the V(C1, C2) basin up to 6.3 and 5.3% at TS **A** and TS **B**, respectively. Furthermore, populations at disynaptic basins V(C2, C3), V(C3, C4), V(C4, C5), V(C5, C6), and V(C6, X7) are respectively 3.43e, 2.47e, 3.19e, 2.44e, and 2.71e for TS **A**, 3.19e, 2.66e, 2.86e, 2.78e, and 2.07e for TS **B**, and 3.64e, 2.52e, 3.09e, 2.52e, and 3.14e for TS **C**. This is qualitatively in agreement with the expected change in the corresponding bond orders in these regions along the electrocyclization reaction depicted in Scheme 1. Note also that the V(C1, C2) valence populations remain centered at 3.81e, 3.85e, and 3.60e for TS **A**, TS **B**, and TS **C**, respectively. These values are close to the expected value of 4.00e, and deviations are associated mainly with fluctuations in the nitrogen lone pair region (5.1%) at TS **A**, the oxygen lone pairs (4.6%) at TS **B**, and the V(C7, H) disynaptic region (4.7%) at TS **C**. This pattern of fluctuation in connection with the examination of nuclear motion along the corresponding imaginary frequencies at the TS requires us to describe these processes as disrotatory pericyclic electrocyclizations.

The ELF constitutes a very simple tool for the description of the electronic rearrangement along these thermal reactions. It can be seen that the lack of cyclic orbital overlap in pseudopericyclic reactions, as exemplified before in the case of thermal decarbonylations,[9] cannot be found in the present study. The specific pattern of electron fluctuation in TS **A**, TS **B**, and TS **C** is described essentially as a cyclic delocalization without differences between the three cases. The fluctuation pattern at the reaction center and the topology of bonding results seem to be very similar in the three cases. Furthermore, this cyclic, although asymmetric, electron fluctuation between the ELF

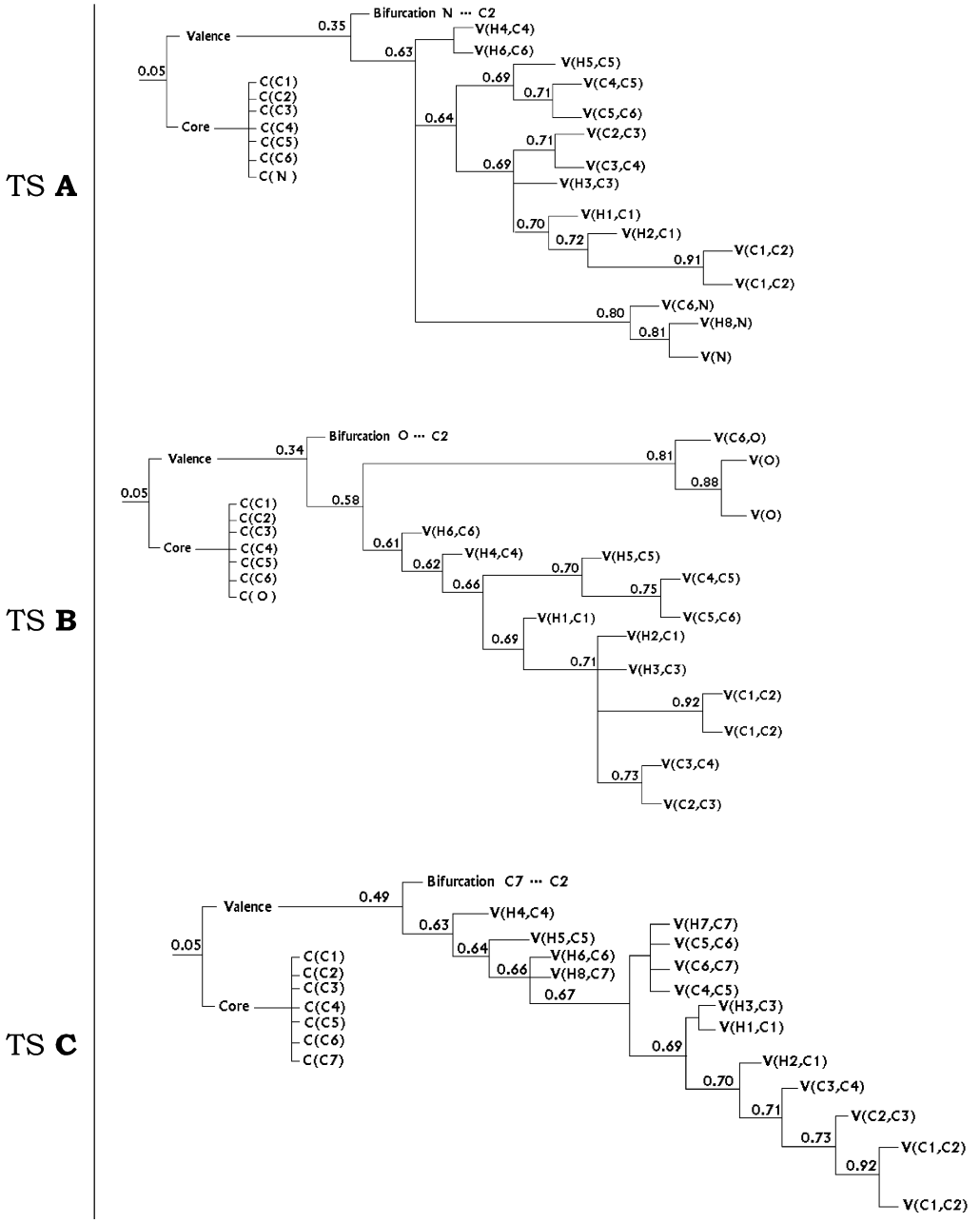

Figure 2. Bifurcation diagrams corresponding to the electron localization function (ELF) analysis at TS **A**, TS **B**, and TS **C** transition states from the optimized wave functions at the B3LYP/6-31+G(d) level of theory.

basins can also be straightforwardly analyzed in light of the reduction of localization domains and bifurcation diagrams. Figure 1 depicts ELF isosurfaces corresponding to 0.84 (i.e., high localization), 0.40, and 0.04 (i.e., delocalization) for TS **A**, TS **B**, and TS **C**. The corresponding bifurcation diagrams are depicted in Figure 2. It is therefore clear that the separation of the valence region at the X7 center from the valence region at the C2 center is located at low ELF values of 0.35, 0.34, and 0.49 for TS **A**, TS **B**, and TS **C**, respectively. This could be interpreted in light of the covariance analysis in terms of the early pericyclic character of electrocyclization at the transition-state position. Moreover, the complete fluctuation pattern reported in Tables 1−3 and Figure 2 reveals the pronounced asymmetric bond-breaking/bond-formation nature of the three electronic rearrangements of this type of electrocyclic process. For instance, the corresponding fluctuations along the cyclic chain domains V(N) → V(C2,C3) → V(C3, C4) → V(C4, C5) → V(C5, C6) → V(C6, N) → V(N) in TS **A** account for 6.0, 25.0, 17.4, 24.6, 15.0, and 33.6%, respectively. It is clear that the opposite trend, V(N) → V(C6,N) → ... → V(N), becomes nearly equivalent (i.e., 32.1, 17.2, 19.9, 20.9, 20.0, and 7.0%). In the TS **B**, the corresponding fluctuations along the domains V(O) → V(C2, C3) → V(C3, C4) → V(C4, C5) → V(C5, C6) → V(C6, O) → V(O) account for 4.8, 25.1, 17.9, 24.4, 13.2, and 25.8%, respectively, with the opposite trend, V(O) → V(C6,O) → ... → V(O), being also equivalent (i.e., 26.2, 12.0, 23.9, 18.6, 22.3, and 5.7%). Close resembling TS **A** and TS **B**, in the case of TS **C**, the corresponding fluctuations along the domain V(C6, C7) → V(C2, C3) → V(C3, C4) → V(C4, C5) → V(C5, C6) → V(C6, C7) account for 5.4, 24.2, 18.6, 22.4, and 18.1%, respectively, and the fluctuation in the opposite domain direction V(C6, C7) → V(C5, C6) → ... → V(C6, C7) account for 21.8, 19.0, 21.7, 18.5, and 5.9%. For these pericyclic processes, the fluctuation of electron density is essentially equivalent both in magnitude and direction for the three transition states.

Moreover, a simple scheme of charge additivity from the basin populations (without including covariance data) shows that in the V(C1, C2) region there is only a very small accumulation of electrons (i.e., 0.12e, 0.10e, and 0.05e for TS **A**, TS **B**, and TS **C**, respectively), which is also consistent for pericyclic processes via TS1 as depicted in Scheme 1. This is in agreement with the arguments that were first discussed by Rodriguez-Otero and Cabaleiro-Lago.[2a,5]

Concluding Remarks

In summary, the topological analysis of ELF, a measure of local Pauli repulsion and an orbital-independent technique for bonding analysis, has been used to explore the nature of bonding at the transition states of the thermal electrocyclization of (*Z*)-1,2,4,6-heptatetraene (**C**) and its heterosubstituted analogues, (2*Z*)-2,4,5-hexatrienal (**B**) and (2*Z*)-2,4,5-hexatrien-1-imine (**A**). The ELF picture of bonding reveals pericyclic disrotatory electrocyclization via transition state TS1 as it is represented in Scheme 1.[2a] This conclusion straightforwardly arises from the fluctuation (i.e., interpreted as electron delocalization) in electron density associated directly with the cyclic reaction center upon the formation of the new C2−X7 bond. As was previously noted from the analysis of other pericyclic[11] and pseudopericyclic transition states,[9] we suggest that the ELF picture of bonding gives a simple, clear, and unequivocal description of the intimate bonding nature of these transition structures.

Acknowledgment. This work has been supported by Fondecyt (grant no. 1030173), by Universidad Andrés Bello (grant UNAB DI-11-02), and by the Spanish Dirección General de Investigación, Ministerio de Ciencia y Tecnología (grant no. BQU2000-1499). We also thank CONICYT and C.S.I.C. for the joint project (no. 2003CL0026).

References and Notes

(1) De Lera, A. R.; Alvarez, R.; Lecea, B.; Torrado, A.; Cossío, F. P. *Angew. Chem., Int. Ed.* **2001**, *40*, 557.

(2) (a) Rodríguez-Otero, J.; Cabaleiro-Lago, E. M. *Angew. Chem., Int. Ed.* **2002**, *41*, 1147. (b) De Lera, A. R.; Cossío, F. P. *Angew. Chem., Int. Ed.* **2002**, *41*, 1150.

(3) See, for instance, (a) Katcher, J.; Fabian, W. M. F. *Theor. Chem. Acc.* **2003**, *109*, 195. (b) Cabaleiro-Lago, E. M.; Rodriguez-Otero, J.; Hermida-Ramon, J, J. M. *J. Phys. Chem. A* **2003**, *107*, 4962. (c) Shelkov, R.; Nahmany, M.; Melman, A. *J. Org. Chem.* **2002**, *67*, 8975. (d) Zhou, C.; Birney, D. M. *J. Am. Chem. Soc.* **2002**, *124*, 5231. (e) Shumway, W. W.; Dalley, N. K.; Birney, D. M. *J. Org. Chem.* **2001**, *66*, 5832. (f) Birney, D. M. *J. Am. Chem. Soc.* **2000**, *44*, 10917. (g) Birney, D. M.; Xu, X. L.; Ham, S. *Angew. Chem., Int. Ed.* **1999**, *38*, 189. (h) Ham, S.; Birney, D. M. *Tetrahedron Lett.* **1997**, *38*, 5925. (i) Birney, D. M.; Ham, S.; Unruh, G. R. *J. Am. Chem. Soc.* **1997**, *119*, 4509. (j) Ham, S.; Birney, D. M. *J. Org. Chem.* **1996**, *61*, 3962.

(4) (a) Schleyer, P. von R.; Maerker, C.; Dransfeld, A.; Jiao, H.; Hommes, N. J. R. v. E. *J. Am. Chem. Soc.* **1996**, *118*, 6317. (b) Cossío, F. P.; Morao, I.; Jiao, H.; Schleyer, P. von R. *J. Am. Chem. Soc.* **1999**, *121*, 6737. (c) Morao, I.; Cossío, F. P. *J. Org. Chem.* **1999**, *64*, 1868.

(5) Rodriguez-Otero, J.; Cabaleiro-Lago, E. M. *Chem.—Eur. J.* **2003**, *9*, 1837.

(6) Birney, D. M. *J. Org. Chem.* **1996**, *61*, 243.

(7) Becke, A. D.; Edgecombe, K. E. *J. Chem. Phys.* **1990**, *92*, 5397.

(8) (a) Savin, A.; Nesper, R.; Wengert, S.; Fässler, T. F. *Angew. Chem., Int. Ed.* **1997**, *36*, 1808. (b) Marx, D.; Savin, A. *Angew. Chem., Int. Ed.* **1997**, *36*, 2077. (c) Savin, A.; Becke, A. D.; Flad, J.; Nesper, R.; Preuss, H.; von Schnering, H. *Angew. Chem., Int. Ed.* **1991**, *30*, 409. (d) Silvi, B.; Savin, A. *Nature* **1994**, *371*, 683. (e) Savin, A.; Silvi, B.; Colonna, F. *Can. J. Chem.* **1996**, *74*, 1088. (f) Noury, S.; Colonna, F.; Savin, A.; Silvi, B. *J. Mol. Struct.* **1998**, *540*, 59.

(9) Chamorro, E. *J. Chem. Phys.* **2003**, *118*, 8687.

(10) Burdett, J. K.; McCormick, T. A. *J. Phys. Chem. A* **1998**, *102*, 6366.

(11) (a) Chamorro, E.; Santos, J. C.; Gómez, B.; Contreras, R.; Fuentealba, P. *J. Chem. Phys.* **2001**, *114*, 23. (b) Chamorro, E.; Santos, J. C.; Gómez, B.; Contreras, R.; Fuentealba, P. *J. Phys. Chem. A* **2002**, *106*, 11533.

(12) Frisch, M. J.; Trucks, G. W.; Schlegel, H. B.; Scuseria, G. E.; Robb, M. A.; Cheeseman, J. R.; Zakrzewski, V. G.; Montgomery, J. A., Jr.; Stratmann, R. E.; Burant, J. C.; Dapprich, S.; Millam, J. M.; Daniels, A. D.; Kudin, K. N.; Strain, M. C.; Farkas, O.; Tomasi, J.; Barone, V.; Cossi, M.; Cammi, R.; Mennucci, B.; Pomelli, C.; Adamo, C.; Clifford, S.; Ochterski, J.; Petersson, G. A.; Ayala, P. Y.; Cui, Q.; Morokuma, K.; Malick, D. K.; Rabuck, A. D.; Raghavachari, K.; Foresman, J. B.; Cioslowski, J.; Ortiz, J. V.; Stefanov, B. B.; Liu, G.; Liashenko, A.; Piskorz, P.; Komaromi, I.; Gomperts, R.; Martin, R. L.; Fox, D. J.; Keith, T.; Al-Laham, M. A.; Peng, C. Y.; Nanayakkara, A.; Gonzalez, C.; Challacombe, M.; Gill, P. M. W.; Johnson, B. G.; Chen, W.; Wong, M. W.; Andres, J. L.; Head-Gordon, M.; Replogle, E. S.; Pople, J. A. *Gaussian 98*, revision A.9; Gaussian, Inc.: Pittsburgh, PA, 1998.

(13) Noury, S.; Krokidis, X.; Fuster, F.; Silvi, B. *TopMoD*; Universite Pierre et Marie Curie: Paris, France, 1997.

(14) Noury, S.; Krokidis, X.; Fuster, F.; Silvi, B. *Comput. Chem.* **1999**, *23*, 597.

(15) (a) Hibbard, B.; Kellum, J.; Paul, B. *Vis5d 5.1, Visualization Project*, 1999; University of Winconsin-Madison Space Science and Engineering Center (SSEC). (b) Hibbard, B.; Santek, D. *Proc. IEEE Visualization '90* **1990**, 129.

(16) Bader, R. F. W. *Localization and Delocalization in Quantum Chemistry*; Chalvet, O. et al., Eds.; Reidel: Dordrecht, The Netherlands, 1975; Vol. 1.

(17) For recent applications, see, for instance, (a) Jorgens, S.; Johrendt, D.; Mewis, A. *Chem.—Eur. J.* **2003**, *9*, 2405. (b) Pilme, J.; Silvi, B.; Alikhani, M. E. *J. Phys. Chem. A* **2003**, *107*, 4506. (c) Chesnut, D. B. *J. Phys. Chem. A* **2003**, *107*, 4307. (d) Chesnut, D. B. *Heteroat. Chem.* **2003**, *14*, 175. (e) Melin, J.; Fuentealba, P. *Int. J. Quantum Chem.* **2003**, *92*, 381. (f) Lepetit, C.; Silvi, B.; Chauvin, R. *J. Phys. Chem. A* **2003**, *107*, 464. (g) Gajewski, G.; Mierzwicki, K.; Latajka, Z. *Chem. Phys. Lett.* **2003**, *369*, 139. (h) Berski, S.; Andres, J.; Silvi, B.; Domingo, L. R. *J. Phys. Chem. A* **2003**, *107*, 601. (i) Chamorro, E.; Fuentealba, P.; Savin, A. *J. Comput. Chem.* **2003**, *24*, 496.

(18) Silvi, B. *J. Phys. Chem. A* **2003**, *107*, 3081. (b) Silvi, B. *Phys. Chem. Chem. Phys.* **2004**, *6*, 256.